Applied Energy xxx (xxxx) xxxx

Contents lists available at ScienceDirect

Applied Energy

journal homepage: www.elsevier.com/locate/apenergy

Wind power forecasting based on singular spectrum analysis and a new hybrid Laguerre neural network

Cong Wang, Hongli Zhang*, Ping Ma

School of Electrical Engineering, Xinjiang University, Urumqi, Xinjiang 830047 China

HIGHLIGHTS

- SAA and data conversion are used to analyze the wind power series.
- A new Laguerre orthogonal basis function in $(-\infty, 0]$ is proposed and verified.
- A innovate hybrid model is proposed to forecast multi-step ahead wind power.
- The OTSTA can increase the prediction accuracy through optimized model parameters.

ARTICLE INFO

Keywords:
Wind power prediction
Hybrid Laguerre neural network
Singular spectrum analysis
Opposition transition state transition algorithm

ABSTRACT

Given the intermittency and randomness of wind energy, the mass grid connection of wind power poses great challenges in power system and increases the threat in power system balance. Wind power forecasting can predict the fluctuation of output wind power in wind farms, which can effectively reduce wind power uncertainty. Improving the accuracy of wind power is indispensable for enhancing the efficiency of wind power utilization. To improve the forecasting accuracy, this research proposed a novel wind power forecasting method based on singular spectrum analysis and a new hybrid Laguerre neural network. First, singular spectrum analysis was used to analyze the wind power series, which decomposes the series into two subsequences, namely, trend and harmonic series and noise series. Then, Laguerre neural network and new Laguerre neural network were proposed to build the hybrid forecasting model optimized by the opposition transition state transition algorithm. The two decomposed signals were used for forecasting the future wind power value by using a forecasting model. Finally, the proposed hybrid forecasting method was investigated with respect to the wind farm in Xinjiang, China. Prediction performance results demonstrated that the proposed model has higher accuracy than the Laguerre neural network, hybrid Laguerre neural network, hybrid Laguerre neural network with singular spectrum analysis, hybrid Laguerre neural network with opposition transition state transition algorithm and singular spectrum analysis, and other popular methods.

1. Introduction

Efficient, clean, and low carbon has become the mainstream of the world's energy development direction. Wind energy, as one of the most popular renewable clean energies, has developed rapidly in recent years. The total installed capacity of 14 years (from 2005 year to 2018 year) is reported in Fig. 1.

It can be seen from Fig. 1 that the wind power installed capacity maintains sustained growth state in recent years, indicating that wind energy utilization remains rapidly increasing. The overall capacity of all wind turbines installed worldwide by the end of 2018 reached 597 GW [1].

Given the intermittency and randomness of wind energy, the mass grid connection of wind power poses great challenges in power system and increases the threat in power system balance. Wind power forecasting is a technology for predicting the fluctuation of output wind power in wind farms, which can effectively reduce wind power uncertainty. In other words, the accuracy of wind power forecasting is the basis of wind system optimization scheduling and efficient accommodation [2]. Improving the forecasting accuracy of wind power is indispensable for enhancing the efficiency of wind power utilization [3]. In general, wind power prediction is based on wind farm information, historical operation data, observed meteorological data, or numerical weather prediction (NWP) data, through data mining

* Corresponding author.
E-mail address: xjdqxy@foxmail.com (H. Zhang).

https://doi.org/10.1016/j.apenergy.2019.114139
Received 19 August 2019; Received in revised form 26 October 2019; Accepted 11 November 2019

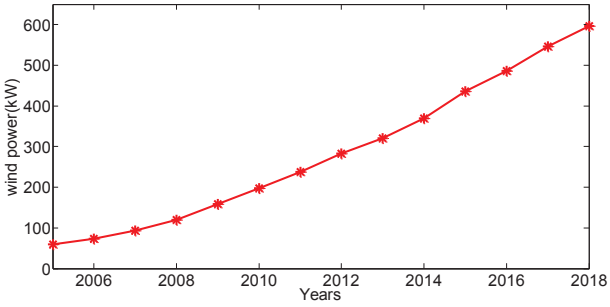

Fig.1. Total installed wind power from 2005 to 2018 worldwide.

technology for the construction of a prediction model. Then the historical data as the input of the model, the future wind power within a period will be gotten by the output of the model.

1.1. Existing wind power forecasting approaches

To increase the accuracy of wind power forecasting, many researchers and utilities have proposed various forecasting methods, including physical and statistical approaches [4]. Physical forecasting methods always build forecasting models via detailed physical description. They differ in how the grids are structured and scaled and how numerical computations are performed [5]. These methods require considerable physical information of the wind farm and its surroundings, which increases the difficulty of prediction. Statistical forecasting methods use the relation between wind power forecasting and explanatory variables, including NWPs and online measured data [6]. Statistical approaches include the conventional statistical approach [7], artificial neural network approach (ANN) [8], ANN–fuzzy approach [9], and others [5]. Statistical wind power forecasting methods can directly describe the nonlinear relationship between input data (as wind power, wind speed and others) and output data (wind power) by analyzing the statistical laws of wind power. Statistical forecasting approaches only use historical data as inputs and can increase the forecasting accuracy, thereby outperforming physical methods for short-term horizon forecasting. In recent years, statistical methods have been popularly used in wind power systems.

With the development of statistical methods, a new branch of the statistical approach called combined or hybrid approach has been presented to improve the accuracy of wind power forecasting, which involves hybrid forecasting models with a combination of different individual models [10]. These methods mainly combine the advantages of several methods to improve the prediction accuracy. Sharifian [11] proposed an intelligent forecasting method for the medium and long-term wind power. A hybrid Type-2 fuzzy neural network was proposed based on fuzzy system, the neural network and PSO algorithm. The effectiveness and applicability of the forecasting method in a power system control center was validated, yielding an RMSE of only 14.85%. Lin [12] presented a multimodel combination method, which combined sparse Bayesian learning, kernel density estimation, and beta distribution estimation. The simulations demonstrated that this combination method has adaptivity and robustness on probabilistic forecasting for different wind farms. Wang [13] constructed analytical conditional distributions of forecast errors based on Gaussian mixture model. Historical data were used to verify the accuracy of the proposed probabilistic models. The MAE of proposed method was 0.3542 for day-ahead forecasting. López [14] presented an new forecasting method combines the long short-term memory and echo state network. Two steps were used to train the forecasting model. This proposal had three advantages, and the experimental results verified that LSTM + ESN combines the characteristics of both networks and obtains a robust estimate of the expected target. Wang [15] proposed the heteroscedastic spline regression model (HSRM) and robust spline regression model (RSRM) to obtain further accurate power curves. These models were optimized using variational Bayesian. HSRM can model power curves with data contaminated by inconsistent samples, and RSRM can model the error distribution with long tail. These two models can obtain satisfactory power forecasts. Afshari [16] used the wavelet transform, neural network (NN), and improved krill herd optimization algorithm (IKHOA) to propose a novel hybrid intelligent method. The novel hybrid intelligent method considers the nonstationary and chaotic nature of the wind generation time series to improve the effectiveness of the forecasting model. The numerical results authenticated the validity of the proposed novel hybrid intelligent method. Jiao [17] combined stacked auto-encoders (SAE) and the backpropagation (BP) algorithm to propose a novel hybrid forecasting method. The model had two phases: pre-training and fine-tuning processes. SAE was used to extract the characteristics from the reference data sequence, whereas the BP algorithm was used to fine-tune the weights of the entire network. The experimental results verified that the method improved the accuracy to 12%. Zjavka [18] used the polynomial decomposition of the general differential equation method to forecast wind power. The designed method using the inverse Laplace transformation aimed at the formation of stand-alone spatial derivative models. The proposed intraday multistep predictions were more precise than those based on middle-term numerical forecasts. Yu [19] proposed an improved long short-term memory-enhanced forget-gate network forecasting model. This model enhanced the effect of forget-gate and changed the activation function to optimize convergence speed. The results showed that the method with spectral clustering has a higher accuracy with an increase of 18.3% than those of other forecasting models. Niu [20] proposed a model of wavelet decomposition (WD) and weighted random forest (WRF) optimized by the niche immune lion algorithm (NILA-WRF) to forecast wind power. The WD-NILA-WRF model combines the advantage of each single model, which uses WD for signal de-noising and the niche immune lion algorithm (NILA) to improve model optimization efficiency. Two empirical analyses were conducted to prove the accuracy of the model, and the experimental results verified the proposed model's validity and superiority.

These hybrid methods improve the wind power forecasting accuracy. Considering that accurate wind power forecasting is a key task in the planning and operation of wind energy generation, increasing the accuracy of wind power forecasting methods remains an important research field. Recently, many feature selection or feature engineering methods and signal processing methods have been introduced to enhance forecasting accuracy. They first analyze data and then use hybrid forecasting methods to predict wind power. Subsequently, data features are extracted or broken down, and the precision is greatly improved. Zhang [10] used the signal filtering technique called singular spectrum analysis (SSA) to analyze the wind power data, and subsequence series were forecasted using different forecasting strategies with support vector machines (SVMs) optimized by the cuckoo search algorithm. Zhang and Zhang [21] used SSA to decompose the original wind power series into the trend and fluctuation components. The trend component was forecasted using least squares SVM, whereas the fluctuation component was forecasted using the deep belief network. SSA can divide the original wind power series into the trend and fluctuation components, which can capture the hidden complicated nature of wind power series in the trend and fluctuation components with different time-frequency scales. Forecasting models are used to predict these subsequences for increasing prediction precision, which can indirectly increase the final prediction accuracy. Lu [22] first used ensemble empirical mode decomposition–permutation entropy to decompose the original wind power series into several subsequences with evident complexity differences. The subsequences were forecasted using least squares SVM. Naik [23] applied variational mode decomposition (VMD) to decompose the original wind power time series data and prevent the mutual effects among different modes. Subsequently, the performance of wind power forecasting was improved. Du [24]

proposed an improved complete ensemble empirical mode decomposition with adaptive noise technology to decompose the wind power time series, which can eliminate noise and extract the main features of the original wind power series. Then, wavelet neural network was used to forecast wind power. The simulation results showed that the method has highly accurate and stable forecasts. Zhou [25] used extreme-point symmetric mode decomposition (ESMD) to decompose wind power into several intrinsic mode functions (IMFs) and one residual (R). For every IMF, extreme learning machine and particle swarm optimization were used for prediction. They verified that the proposed method has more robust and accurate forecasting results than other methods. The EEMD, VMD, CEEMD, and ESMD are tools for decomposing wind power into several intrinsic mode functions. These intrinsic mode functions have different characteristics scales. Wang [26] selected NWP data as the inputs of the proposed deep belief network (DBN) forecasting model. To select the effectiveness samples, the authors used k-means clustering algorithm to analyze a large amount of data. Cluster analysis refers to the process of grouping a collection of physical or abstract objects into multiple classes of similar objects, which can divide the samples into several disjoint subsets. The k-means clustering algorithm has strong dependence on the beginning clustering center. Hence, the selection results will directly affect the clustering effect. Leng [27] applied a ridgelet transform to decompose a wind signal into sub-signals. The output of the ridgelet transform is regarded as the input of new feature engineering to identify the best candidates to be used as the input of a new hybrid closed loop forecast engine. Ridgelet transform can obtain good result for linear image detection but cannot satisfy the requirements of curvilinear singularity detection.

These proposed hybrid models consist of feature selection or feature engineering methods, optimization stage, and forecasting stage, which can improve the accuracy and stability of wind power forecasting. Nevertheless, most of these methods have drawbacks. For instance, EMD and WD lack a clear physical meaning and strict mathematical theories, and DBN needs a large amount of sample data. Accurate wind power prediction results are important for the rapid implementation of power generation scheduling plans and instructions [28]. Hence, effective forecasting methods should be developed for wind power series.

1.2. The novelty of this study

The present research proposed a novel, new hybrid wind power forecasting method based on SSA and a new hybrid Laguerre neural network (HLNN). This process involves the three following steps:

Step 1: SSA is used to analyze the wind power series, which decomposes the series into two subsequences.

Step 2: A new hybrid Laguerre neural network is proposed to build the hybrid wind power forecasting model optimized by the opposition transition state transition algorithm (OTSTA). The hybrid model has two sections: type I and type II forecasting models for forecasting positive and negative series.

Step 3: The proposed hybrid forecasting method is subsequently investigated with respect to the wind farm in Xinjiang, China. The prediction performance results demonstrate that the proposed model (OTSTA-SSA-HLNN) has higher accuracy than LNN, HLNN, SSA-HLNN, state transition algorithm (STA)-SSA-HLNN, and other benchmark models, such as radial basis function (RBF), extreme learning machine (ELM), support vector regression (SVR), and wavelet neural networks (WNN).

The main novelty and innovation contributions of OTSTA-SSA-HLNN are described as follows:

(1) Data-processing stage: First, the SSA is used to decompose series into two subsequences, namely, trend and harmonic series and noise series, by reconstructing the original wind power series. The wind power series can be divided into the trend and fluctuation components series, which is conducive for learning the characteristics of the power series. Second, unlike in common studies, we calculate the positive and negative conversions of two series.

(2) Laguerre polynomial and neural network are used to build a new LNN forecasting model. Considering that the Laguerre orthogonal basis function is limited to $[0, +\infty)$, we propose a new negative orthogonal basis function in$(-\infty, 0]$. Then, we use these two Laguerre orthogonal functions to build a hybrid forecasting method. The hybrid model has two sections: type I and type II forecasting models for forecasting positive and negative series. The hybrid model not only combines the advantages of neural network and Laguerre polynomial (or negative Laguerre polynomial) but also deeply considers the features of the data. The use of forecasting model for forecasting positive and negative series will improve the forecasting accuracy.

(3) OTSTA is proposed to optimize the weights of hybrid forecasting method, which avoids the selection of parameters. A local optimal discriminant mechanism is used to judge whether a premature phenomenon occurred. If the algorithm results in precocious phenomena, an opposition transition learning mechanism is proposed to let algorithm jump out earliness state. OTSTA not only has few parameters and simple structure but also has good convergence, which can indirectly improve wind power forecasting accuracy and improve the model's stability.

(4) To obtain effective forecasting results and improve its practical application value, this study not only analyzes the results with multi-input but also verifies the prediction capability of multi-step ahead wind power prediction to protect the operation of wind power systems effectively.

1.3. Structure of this paper

This paper is designed as follows: Section 2 shows the basic methods, such as SSA, OTSTA, and HLNN, used for the proposed model. Section 3 describes the framework of the novel hybrid forecasting model for wind power system. Section 4 presents the experimental results and discussion, and Section 5 provides the conclusion.

2. Proposed methodology

This paper proposes a novel hybrid forecasting model. The proposed basic methods, such as SSA, OTSTA, and HLNN, used for the proposed model are described in this section.

2.1. SSA

SSA, which is combined with multivariate statistics and probability theory, is a nonparametric method for time series analysis. SSA can identify and extract the constituent of trend, periodic oscillation, and noise from original series [29]. SSA includes two stages: embedding and singular value decomposition (SVD) and reconstruction, including grouping and diagonal averaging [30]. The detailed steps are as follows:

(1) **Embedding**. Suppose the wind power series is $Y = [y_1, y_2, \cdots, y_N]$. L is the only parameter, namely, window length, usually $L = {}^{N}/_{2}$. The L-lagged vectors can be defined as $X_i = [y_i, y_{i+1}, \cdots, y_{i+L-1}]$. The following trajectory matrix can be obtained:

$$X = \begin{bmatrix} y_1 & y_2 & \cdots & y_K \\ y_2 & y_3 & \cdots & y_{K+1} \\ \vdots & \vdots & \vdots & \vdots \\ y_L & y_{L+1} & \cdots & y_N \end{bmatrix} \quad (1)$$

(2) **Singular value decomposition.** $S = XX^T$ is the covariance matrix. The SVD is used to produce the eigenvalue $\lambda_1, \lambda_2, \cdots \lambda_L$ and

eigenvector $U_1, U_2, \cdots U_L$. Let, $d = \max\{i\}(\lambda_i > 0)$, and $V_i = X^T U_i \sqrt{\lambda_i}(i = 1, 2, \cdots, d)$, the SVD of X can be described as follows:

$$X = \sum_{i=1} \sqrt{\lambda_i} U_i V_i^T \tag{2}$$

The vectors, namely, principle components, are expressed as V_i.

(3) **Grouping.** Suppose a group of indices $I = [i_1, i_2, \cdots, i_p]$, X_I is defined as $X_I = X_{i1} + X_{i2} + \cdots X_{ip}$. The trajectory matrix is $X = X_{I1} + X_{I2} + \cdots X_{\mathrm{Im}}$.

(4) **Diagonal averaging.** Let Z be a matrix with a dimension of$L \times K$. Set $K* = \max(L, K)$ and $z_{ij}^* = z_{ij}(L < K)$; else $z_{ij}^* = z_{ji}$. Diagonal averaging transfers matrix Z into a series $\{z_1, z_2, \cdots, z_N\}$ via the following equation :

$$y_k = \begin{cases} \frac{1}{k}\sum_{q=1}^{k+1} z_{q,k-q+1}^* & 1 \leqslant k \leqslant L^* \\ \frac{1}{L^*}\sum_{q=1}^{L^*} z_{q,k-q+1}^* & L^* \leqslant k \leqslant K^* \\ \frac{1}{N-K+1}\sum_{q=k-K*+1}^{N-K^*+1} z_{q,k-q+1}^* & K^* \leqslant k \leqslant N \end{cases} \tag{3}$$

2.2. HLNN

2.2.1. Laguerre orthogonal basis function

Laguerre polynomial is proposed by Edmond Laguerre, which is a column orthogonal polynomial in the nonnegative real number set, and is associated with the Gamma distribution density function.

Definition. The Laguerre polynomial can be described as follows:

$$L_n(x) = e^x \frac{d^n}{dx^n}(x^n e^{-x})\ x \in [0, +\infty) \tag{4}$$

The Laguerre polynomial has orthogonality about weight function, as follows:

$$\int_0^\infty e^{-x} L_n(x) L_m(x) dx = \begin{cases} 0, & m \neq n \\ (n!)^2, & m = n \end{cases} \tag{5}$$

Its recurrence relation is shown as follows:

$$\begin{cases} L_0(x) = 1, \\ L_1(x) = 1 - x, \\ L_{n+1}(x) = (1 + 2n - x)L_n(x) - n^2 L_{n-1}(x)\ (n = 1, 2, \cdots) \end{cases} \tag{6}$$

On the basis of polynomial theory, the Laguerre orthogonal basis feed-forward neural network is constructed and has been popularly used in recent years [31]. Considering the independent variable definitional domain of Laguerre orthogonal basis function of $[0, +\infty)$, the Laguerre orthogonal basis feed-forward neural network cannot be utilized to solve many actual engineering problems. Methods should be proposed in solving this problem.

2.2.2. New Laguerre orthogonal basis function

To improve the applicability of Laguerre orthogonal basis, our group proposed a new Laguerre polynomial. The independent variable definitional domain of new Laguerre orthogonal basis function is $(-\infty, 0]$.

Definition. The Laguerre polynomial can be described as follows:

$$NL_n(x) = e^{-x} \frac{d^n}{dx^n}(x^n e^x)\ x \in (-\infty, 0] \tag{7}$$

The new Laguerre polynomial has orthogonality about weight function, as follows:

$$\int_{-\infty}^0 e^x NL_n(x) NL_m(x) dx = \begin{cases} 0, & m \neq n \\ (n^2)!, & m = n \end{cases} \tag{8}$$

Its differential equation is as follows:

$$xNL_n^{''}(x) + (x + 1)NL_n'(x) - nNL_n(x) = 0 \tag{9}$$

Its recurrence relation is shown as follows:

$$\begin{cases} NL_0(x) = 1, \\ NL_1(x) = 1 + x, \\ NL_{n+1}(x) = (1 + 2n + x)NL_n(x) - n^2 NL_{n-1}(x)\ (n = 1, 2, \cdots) \end{cases} \tag{10}$$

Proof. Suppose $w(x) = x^n e^x$, the derivative is $w'(x) = nx^{n-1}e^x + x^n e^x$

Hence,

$$xw'(x) - (x + n)w(x) = 0 \tag{11}$$

$$[xw'(x) - (x + n)w(x)]^{(n+1)} = 0 \tag{12}$$

$$xw^{(n+2)}(x) + (1 - x)w^{(n+1)}(x) - (n + 1)w^{(n)}(x) = 0 \tag{13}$$

Considering that $NL_n(x) = e^{-x}\frac{d^n}{dx^n}(x^n e^x)\ x \in (-\infty, 0]$, the following can be obtained:

$$\begin{cases} w^{(n)}(x) = e^x NL_n(x) \\ w^{(n+1)}(x) = e^x[NL'_n(x) + NL_n(x)] \\ w^{(n+2)}(x) = e^x[NL^{'}{}'_n(x) + 2NL'_n(x) + NL_n(x)] \end{cases} \tag{14}$$

By substituting Eq. (14) into Eq. (13), the following can be obtained:

$$xNL_n^{''}(x) + (x + 1)NL_n'(x) - nNL_n(x) = 0 \tag{15}$$

The derivative of Eq (7) is as follows:

$$NL_n'(x) = ne^{-x}(x^{n-1}e^x)^{(n)} \tag{16}$$

Furthermore,

$$(x^n e^x)^{(n)} = [x(x^{n-1}e^x)]^{(n)} = x(x^{n-1}e^x)^{(n)} + n(x^{n-1}e^x)^{(n-1)} \tag{17}$$

The following expression can be obtained:

$$NL_n(x) = e^{-x}(x^n e^x)^{(n)} = (x/n)NL_n'(x) + nNL_{n-1}(x) \tag{18}$$

$$NL_n'(x) = (n/x)NL_n(x) - (n^2/x)NL_{n-1}(x) \tag{19}$$

Hence,

$$xNL_n'(x) = nNL_n(x) - n^2 NL_{n-1}(x) \tag{20}$$

The derivative of Eq. (20) is as follows:

$$NL_n'(x) + xNL_n^{''}(x) = nNL_n'(x) - n^2 NL_{n-1}'(x) \tag{21}$$

The following expression can also be obtained:

$$xN_n^{''}(x) = (n - 1)NL_n'(x) - n^2 NL_{n-1}'(x) \tag{22}$$

$$NL_{n-1}'(x) = [(n - 1)/x]NL_{n-1}(x) - [(n - 1)^2/x]NL_{n-2}(x) \tag{23}$$

By substituting Eqs. (21), (22), and (23) into Eq. (9), the following can be obtained:

$$NL_n(x) = (x + 2n - 1)NL_{n-1}(x) - (n - 1)^2 NL_{n-2}(x) \tag{24}$$

Let $n = n + 1$, Eq (24) can be rewritten as follows:

$$NL_{n+1}(x) = (x + 2n + 1)NL_n(x) - n^2 NL_{n-1}(x) \tag{25}$$

When $m \neq n$, by multiplying both sides of Eq (9) by e^x, the following can be obtained:

$$e^x[xNL_n^{''}(x) + (x + 1)NL_n'(x) - nNL_n(x)] = [xe^x NL_n'(x)]' - ne^x NL_n(x) = 0 \tag{26}$$

By multiplying both sides of Eq. (26) by $NL_m(x)$, the following can be obtained:

$$[xe^{x}NL_n'(x)]'NL_m(x) - ne^{x}NL_n(x)NL_m(x) = 0 \tag{27}$$

On the basis of Rotation symmetric theory, the following can be obtained:

$$[xe^{x}NL_m'(x)]'NL_n(x) - me^{x}NL_m(x)NL_n(x) = 0 \tag{28}$$

Eq (28) minus Eq (27), then do integral operation, the following can be obtained:

$$\begin{aligned}
&(m-n)\int_{-\infty}^{0} e^{x}NL_m(x)NL_n(x)dx \\
&= \int_{-\infty}^{0}\{[xe^{x}NL'_n(x)]'NL_m(x) - [xe^{x}NL'_m(x)]'NL_n(x)\}dx \\
&= [xe^{x}NL'_n(x)NL_m(x) - xe^{x}NL'_m(x)NL_n(x)]_{-\infty}^{0} \\
&\quad - \int_{-\infty}^{0}[xe^{x}NL'_n(x)NL'_m(x) - xe^{x}NL'_m(x)NL'_n(x)]dx \\
&= 0 - 0 \\
&= 0
\end{aligned} \tag{29}$$

When $m = n$, by multiplying both sides of Eq (9) by $NL_{n-1}(x)$ and then performing the integral operation, the following can be obtained:

$$\begin{aligned}
&\int_{-\infty}^{0}[xe^{x}NL'_n(x)]'NL_{n-1}(x)dx - \int_{-\infty}^{0}ne^{x}NL_n(x)NL_{n-1}(x)dx \\
&= [xe^{x}NL'_n(x)NL_{n-1}(x)]_{-\infty}^{0} - \int_{-\infty}^{0}[xe^{x}NL'_n(x)NL'_{n-1}(x)]dx \\
&= 0 - \int_{-\infty}^{0}[xe^{x}NL'_n(x)NL'_{n-1}(x)]dx = 0
\end{aligned} \tag{30}$$

Hence,

$$\int_{-\infty}^{0}[xe^{x}NL'_n(x)'NL'_{n-1}(x)]dx = 0 \tag{31}$$

Moreover,

$$NL_n'(x) = ne^{-x}[(n-1)x^{n-2}e^{x} + x^{n-1}e^{x}]^{(n-1)} = nNL'_{n-1}(x) + nNL_{n-1}(x) \tag{32}$$

By multiplying both sides of Eq. (9) by $NL_n(x)$, performing the integral operation, and substituting Eqs. (31), (32), and (18) into Eq. (9), the following can be obtained:

$$\begin{aligned}
n\int_{-\infty}^{0}e^{x}NL_n^2(x)dx &= \int_{-\infty}^{0}[xe^{x}NL'_n(x)]'NL_n(x)dx \\
&= -\int_{-\infty}^{0}xe^{x}[NL'_n(x)]^2dx \\
&= -\int_{-\infty}^{0}xe^{x}NL'_n(x)[nNL'_{n-1}(x) + nNL_{n-1}(x)]dx \\
&= -n\int_{-\infty}^{0}e^{x}[nNL_n(x) - n^2NL_{n-1}(x)]NL_{n-1}(x)dx \\
&= n^3\int_{-\infty}^{0}e^{x}NL_{n-1}{}^2(x)dx
\end{aligned} \tag{33}$$

Hence,

$$\int_{-\infty}^{0}e^{x}NL_n{}^2(x)dx = n^2\int_{-\infty}^{0}e^{x}NL_{n-1}{}^2(x)dx \tag{34}$$

From above analysis, on the basis of Eqs. (15), (25), (29), and (34), the new Laguerre polynomial has orthogonality about weight function, and its differential equation and recurrence relation are verified. Hence, the new Laguerre polynomial satisfies the requirement of the theory.

2.2.3. Hybrid Laguerre Neural Network

Laguerre polynomial, new Laguerre polynomial, and neural network are used to build a hybrid forecasting method. The hybrid model has two sections, namely, type I forecasting model with Laguerre polynomial as neurons of hidden layer, which is used to forecast positive series, and type II forecasting model with new Laguerre polynomial as neurons of hidden layer, which is used to forecast negative series. Both sections select a three-layer single-input and single-output neural network, as shown in Fig. 2.

The network has a i-q-1 structure. The weight is 1 from the input layer to the hidden layer, and the excitation function in the hidden layer is taken as Laguerre polynomial ($L(\bullet) = [L_0(\bullet), L_1(\bullet), \cdots, L_P(\bullet)]$) or new Laguerre polynomial ($NL(\bullet) = [NL_0(\bullet), NL_1(\bullet), \cdots, NL_P(\bullet)]$), where $p = q$-1.

The input of nerve cells in the hidden layer is as follows:

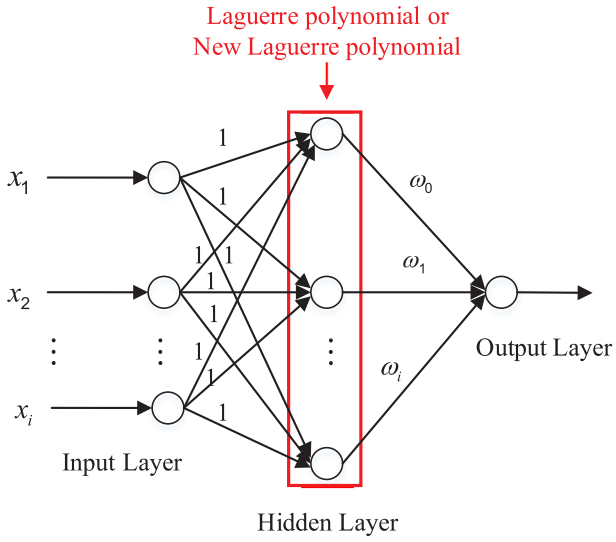

Fig. 2. Neural network of Laguerre and new Laguerre neural networks.

$$net_j = \sum_{m=1}^{i} x_m,\ j = 0,\ 1,\ \cdots, p \tag{35}$$

The output of nerve cells in the output layer is as follows:

$$y = \sum_{j=0}^{p}\omega_j g_j(net_j) \tag{36}$$

where $g_j(net_j)$ is the output of hidden nerve cells.

For the Laguerre orthogonal basis neural network, all points must be adjusted to the positive axis. The wind power series considered is $Y = [y_1, y_2, \cdots, y_N]$ and $y_{\min} = \min\{y_i\}$. A positive dispose to $Y = [y_1, y_2, \cdots, y_N]$ is performed to obtain $y_{t1} = y_i - y_{\min}$.

For the new Laguerre orthogonal basis neural network, all points must be adjusted to the nonpositive axis. The wind power series are assumed as $Y = [y_1, y_2, \cdots, y_N]$ and $y_{\max} = \max\{y_i\}$. A nonpositive dispose to $Y = [y_1, y_2, \cdots, y_N]$ is performed to obtain $y_{t2} = y_i - y_{\max}$.

A hybrid neural network is constructed to combine the advantages of two orthogonal basis neural networks. First, wind power series are adjusted to the nonpositive and positive axes through data conversion. Second, the orthogonal basis neural networks are used to forecast the wind power series. Third, the results of the two models are obtained via inverse conversion. Lastly, the results of the forecasting models are combined and averaged, and the final forecasting results are outputted.

2.3. OTSTA

The state transition algorithm is presented in 2011 [32]. Due to its advantages, such as less parameters, simple structure, easy to understand et ac, STA is popular used in many optimization problems. The defining of state transition is shown as:

$$\begin{cases} x_{k+1} = A_k x_k + B_k u_k \\ y_k = f(x_{k+1}) \end{cases} \tag{37}$$

where $x_k \in R^n$ is a state and corresponds to the optimization problem's solution. $A_k, B_k \in R^{n\times n}$ are state transition matrices, which are also called the operators of optimization algorithm. $u_k \in R^n$ is the function of state x_k. $f(x_k)$ is the objective function. This algorithm has four operators [28], namely, rotation transformation (RT), translational operation (TT), expansion transformation (ET), axesion transformation (AT), and primal dual (PD) approach. These operators are presented in Ref. [33].

To prevent the STA from being trapped in the local optimum during optimization, an improved algorithm, which consists of the following

steps, is proposed:

Step 1: A local optimal discriminant mechanism is used to judge whether the result approaches the local optimum.

Let the fitness variance of STA be as follows:

$$S^2 = \sum_{i=1}^{N} \left(\frac{f(x_i^k) - f_a^k}{\max(\max |f(x_i^k) - f_a^k|, 1)} \right)^2 \tag{38}$$

where f_a^k is the average fitness value of kth. The smaller theS^2, the higher the degree convergence of the algorithm.

If $S^2 < \alpha$ and the theory optimal value is superior to the current fitness optimal value, the algorithm is in its local optimum. α is a positive value, which is set based on the optimization problems.

Step 2: Opposition transition (OT) learning is proposed to solve the local optimal problems of the algorithm.

Definition: $x = (x_1, x_2, \cdots, x_D)$ is a solution in the space of D dimension and $x_i \in [a_i, b_i]$. The reverse solution of $x = (x_1, x_2, \cdots, x_D)$ is $x_i' = (x_1', x_2', \cdots, x_D')$, where $x_i' = -x_i$ and $x_i' \in [a_i, b_i]$.

If the STA is trapped in the local optimum, then the opposition transition is added to the algorithm. On the basis of the probabilistic variation of the reverse solution, the opposition transition operator is as follows:

$$X_i = \begin{cases} \varepsilon x_i + (1 - \varepsilon) x_i', & x_i islocaloptimalsolution \\ x_i, & others \end{cases} \tag{39}$$

where $0 < \varepsilon < 1$.

Fig. 3 shows the detailed flowchart of OTSTA.

3. Architecture of hybrid wind power forecasting model

A novel hybrid forecasting method for wind power is proposed in this paper. Fig. 4 presents the forecasting process of the proposed forecasting model. The entire process is introduced as follows:

Step 1: A wind power dataset measured from the wind farm in Xinjiang is collected.

Step 2: SSA is used to analyze the two wind power series, which are decomposed into two subsequences, namely, trend and harmonic series and noise series by reconstructing the original wind power series.

Step 3: The positive and negative conversions of the two decomposed signals are calculated. The two positive and negative decomposed signals are used to forecast the future wind power value by using the forecasting model.

Step 4: The hybrid wind power forecasting model is used to forecast the wind power series. Type I forecasting model is used to forecast positive trend and harmonic series. Type II forecasting model is utilized to forecast negative trend and harmonic series. In this step, OTSTA is adopted to optimize the forecasting models.

Step 5: The proposed hybrid forecasting method is subsequently investigated with respect to the wind farm in Xinjiang, China. The prediction performance results demonstrate that the proposed model (OTSTA-SSA-HLNN) has higher accuracy than LNN, HLNN, SSA-HLNN, and STA-SSA-HLNN, and other benchmark models, such as RBF, ELM, SVR, and WNN.

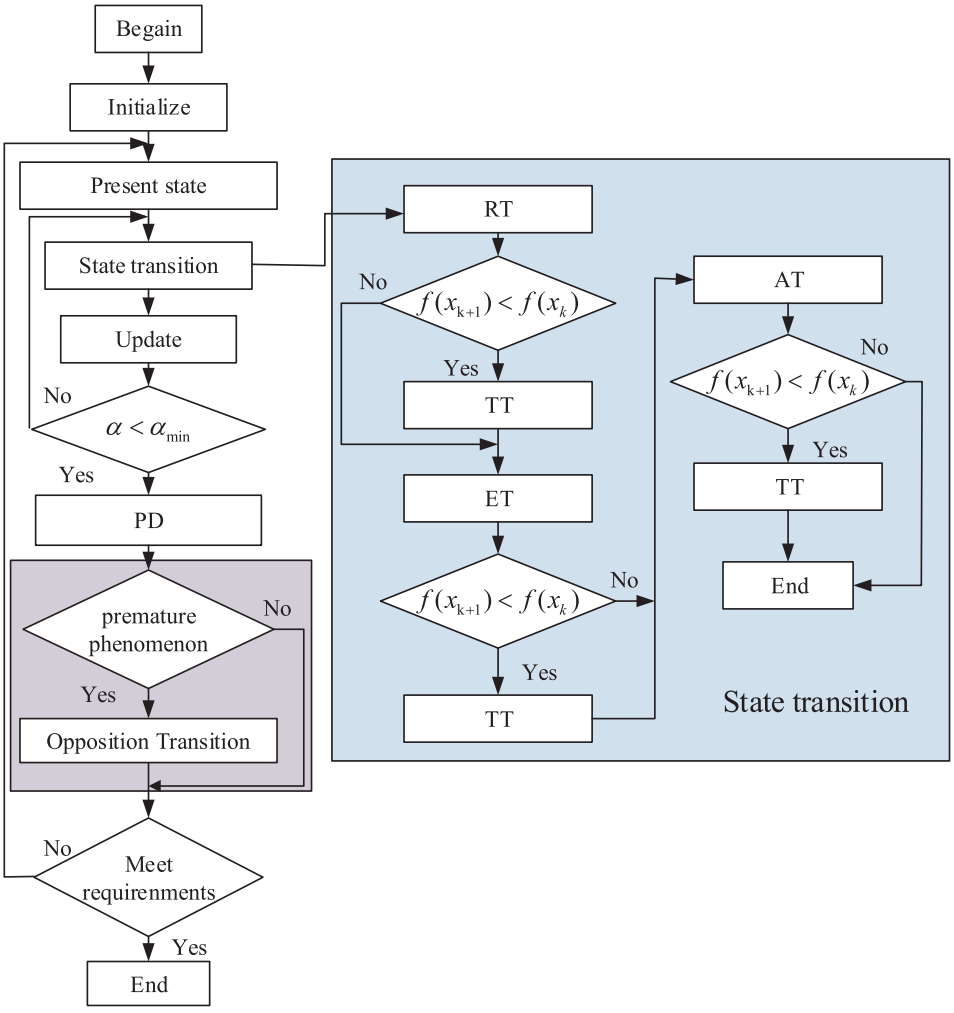

Fig. 3. Detailed flowchart of OTSTA.

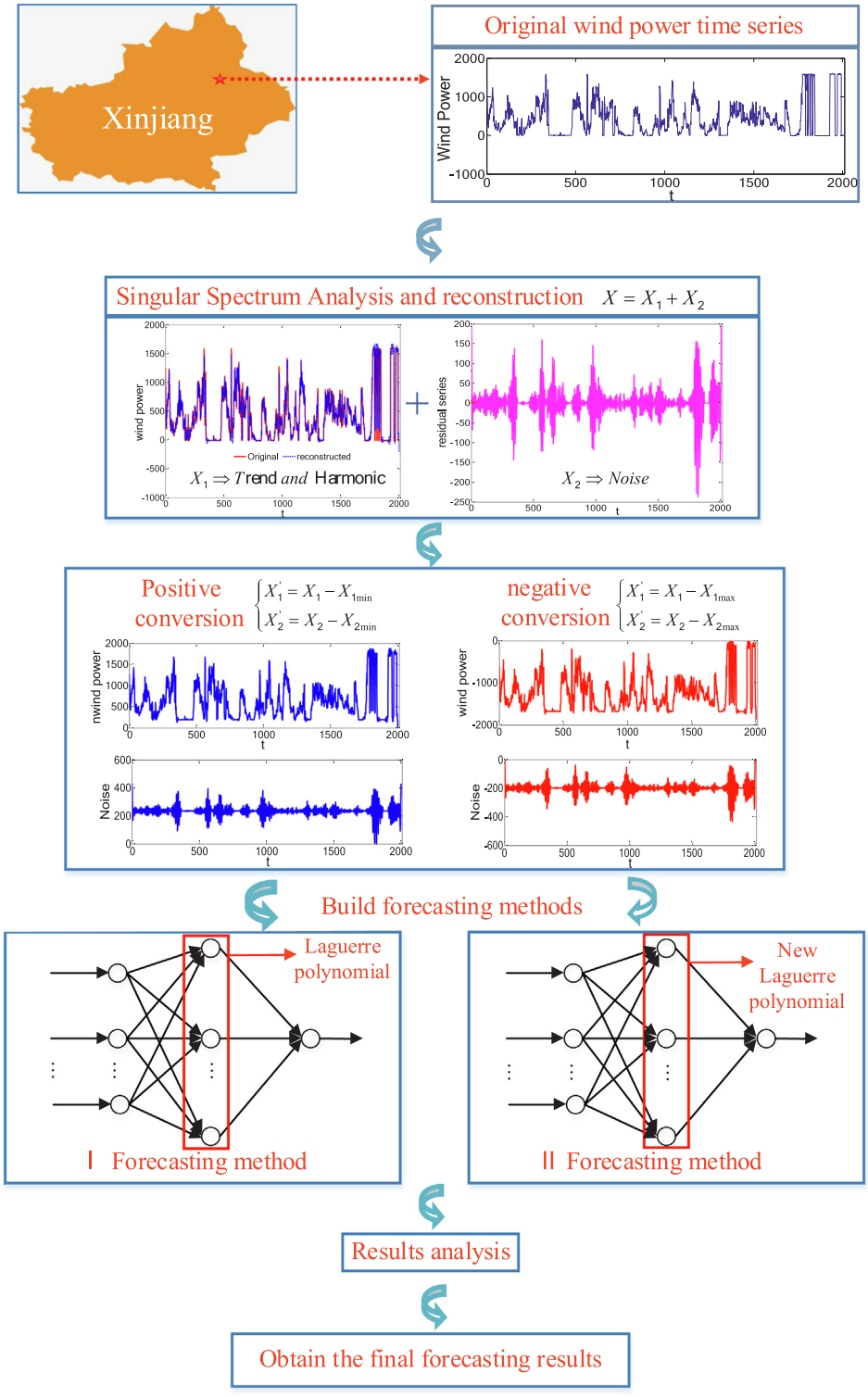

Fig. 4. Detailed forecasting process of the proposed forecasting model.

4. Cases study and analysis

4.1. Performance criteria

The formula for the normalized root mean square error (RMSE) is shown as follows [33]:

$$RMSE = \sqrt{\frac{1}{N}\sum_{i=1}^{N}\left(\frac{y_i - \hat{y}_i}{y_i}\right)^2} \times 100\% \quad i = 1, 2, \cdots, N \tag{40}$$

The formula for the normalized mean absolute error (MAE) is shown as follows [34]:

$$MAE = \frac{1}{N}\sum_{i=1}^{N}\left|\frac{y_i - \hat{y}_i}{y_i}\right| \times 100\% \quad i = 1, 2, \cdots, N \tag{41}$$

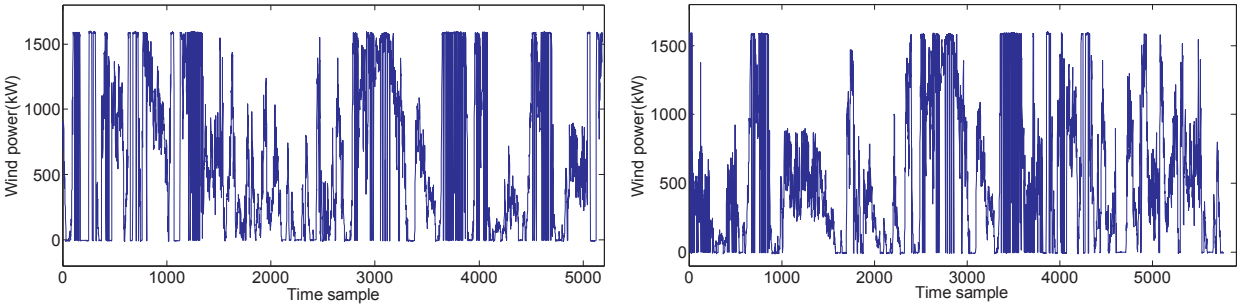

(a) Experiment I samples (b) Experiment II samples

Fig. 5. Experimental samples from Xinjiang, China.

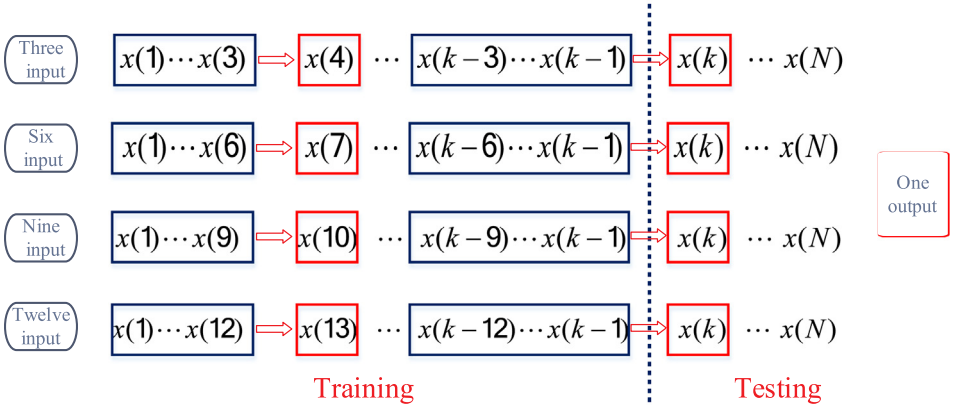

Fig. 6. Forecasting principle.

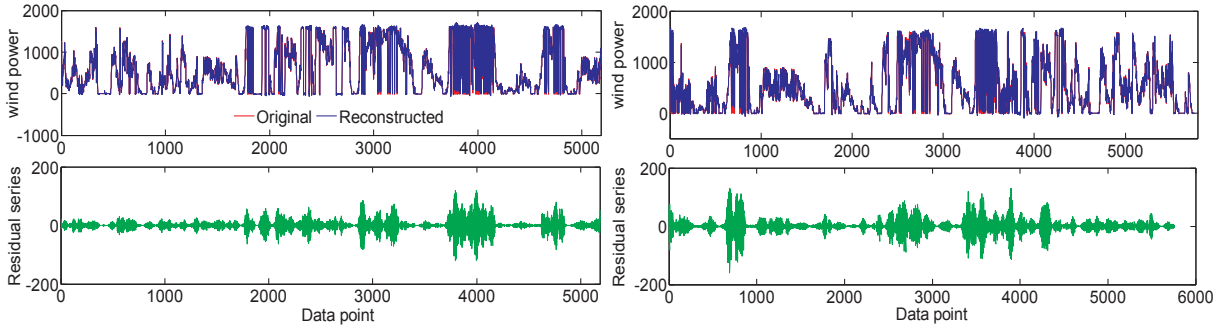

(a) Experiment I samples (b) Experiment II samples

Fig. 7. Time series decomposed.

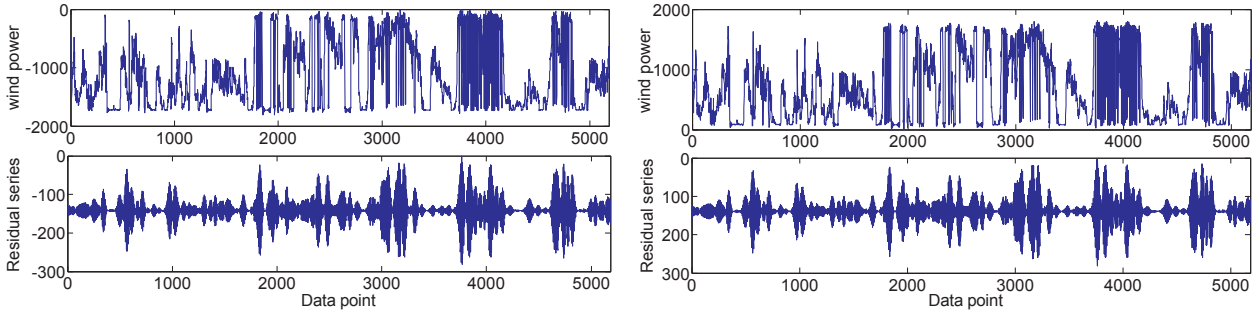

(a) Negative series (b) Positive series

Fig. 8. Results of positive and negative conversion for experiment I.

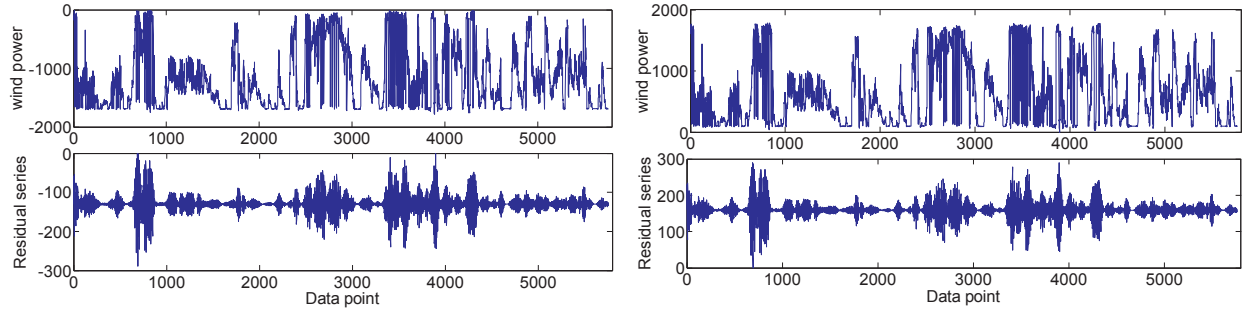

(a) Negative series (b) Positive series

Fig. 9. Results of positive and negative conversion for experiment II.

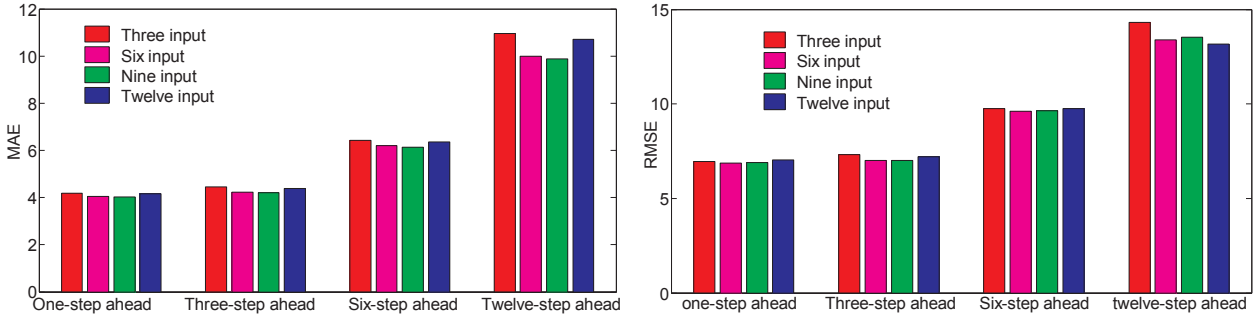

(a) MAE and RMSE histograms of Experiment I

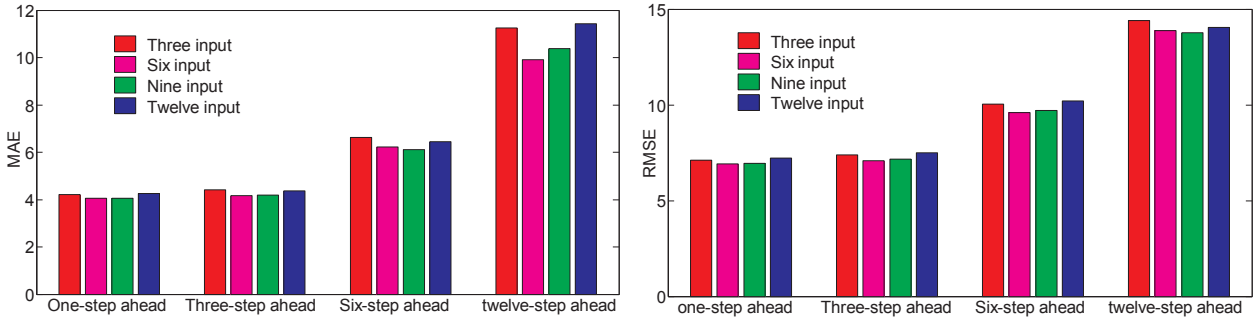

(b) MAE and RMSE histograms of Experiment II

Fig. 10. Forecasting error comparison of proposed models with different inputs.

Table 1
Values for proposed models with different input for various time horizons.

		Error	Three-input	Six-input	Nine-input	Twelve-input
ExperimentI	One-step ahead	MAE(%)	4.1927	4.0495	4.0260	4.1615
		RMSE(%)	6.9613	6.8763	6.9038	7.0327
	Three-step ahead	MAE(%)	4.4609	4.2188	4.1953	4.3776
		RMSE(%)	7.3104	7.0088	7.0236	7.2009
	Six-step ahead	MAE(%)	6.4167	6.1927	6.1276	6.3516
		RMSE(%)	9.7638	9.6154	9.6398	9.7659
	Twelve-step ahead	MAE(%)	10.9505	10.0026	9.8906	10.7214
		RMSE(%)	14.3031	13.4024	13.5387	13.1718
Experiment II	One-step ahead	MAE(%)	4.2024	4.0521	4.0573	4.2582
		RMSE(%)	7.1213	6.9244	6.9436	7.2120
	Three-step ahead	MAE(%)	4.4132	4.1579	4.2011	4.3699
		RMSE(%)	7.4026	7.0752	7.1822	7.4871
	Six-step ahead	MAE(%)	6.6201	6.2123	6.1099	6.4422
		RMSE(%)	10.0429	9.5912	9.7214	10.2025
	Twelve-step ahead	MAE(%)	11.2416	9.9126	10.3893	11.4256
		RMSE(%)	14.4022	13.8812	13.7622	14.0402

Table 2
The errors comparison with different models for various time horizons.

		Error	HLNN	SSA-HLNN	STA-SSA-HLNN	OTSTA-SSA-HLNN
Experiment I	One-step ahead	MAE(%)	6.2396	5.3214	4.1979	4.0495
		RMSE(%)	10.7386	8.0124	7.0926	6.8763
	Three-step ahead	MAE(%)	6.6527	5.6235	4.4561	4.2188
		RMSE(%)	11.4325	9.4985	7.3109	7.0088
	Six-step ahead	MAE(%)	8.8210	6.8320	6.5156	6.1927
		RMSE(%)	12.0216	11.5341	9.8961	9.6154
	Twelve-step ahead	MAE(%)	12.3158	11.2891	10.1482	10.0026
		RMSE(%)	15.9965	15.0031	12.5411	13.4024
Experiment II	One-step ahead	MAE(%)	6.3562	5.4021	4.2413	4.0521
		RMSE(%)	11.8810	8.3124	7.2922	6.9244
	Three-step ahead	MAE(%)	7.0124	5.7275	4.4992	4.1579
		RMSE(%)	11.4231	9.6253	7.9002	7.0752
	Six-step ahead	MAE(%)	9.3923	7.8782	6.5234	6.2123
		RMSE(%)	12.8124	10.6301	10.0234	9.5912
	Twelve-step ahead	MAE(%)	12.1106	11.1923	10.8108	9.9126
		RMSE(%)	15.7165	14.9910	14.1451	13.8812

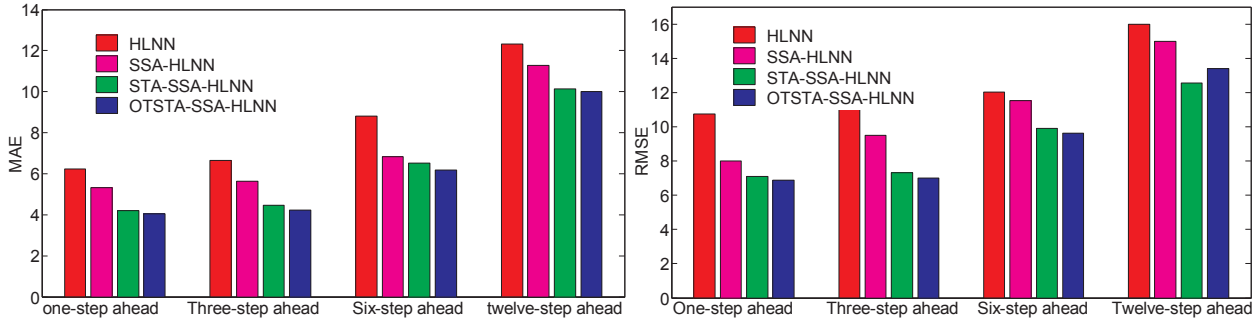

(a) MAE and RMSE histograms of experiment I

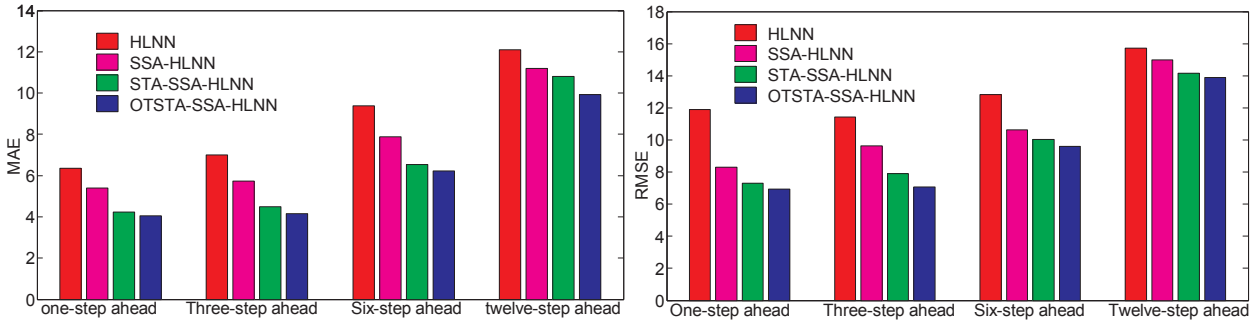

(b) MAE and RMSE histograms of experiment II

Fig. 11. Forecasting error comparison of the proposed models with different inputs.

where N is the number of time series, y_i is the actual value, and $\hat{y}_i$ is the prediction value.

4.2. Data collection

We selected the data from a wind farm in Xinjiang, China, to verify the performance of the proposed model. To analyze the influence of training sample size to the precision of the forecasting model and verify the robustness of the forecasting model, two datasets collected from the wind farms were considered for the experiments. For experiment I, the wind power dataset was collected for the entire year of 2014. Considering various factors, such as seasons, the 5th, 15th, and 25th days of each month were selected as samples. 10-min wind power output data sets' hourly averages were applied for the analysis. The dataset included 5184 samples. A total of 4800 samples were used for training models, and the 384 remaining samples were used for model evaluation. For experiment II, the wind power dataset was collected for the entire year of 2016. Considering various factors, such as seasons, the dataset covers the days from the 1st to the 10th of January, April, July, and October. The dataset included 5760 samples. The training dataset covered the days from the 1st to the 8th of the four months, and the remainder comprised the testing dataset. Fig. 5 shows the samples.

The network has a i-q-1 structure. The appropriate input number of the model can improve the forecasting accuracy. The forecasting strategy with input lengths of i = 3, 6, 9, and 12 was also applied to evaluate the performance of the proposed mode, as shown in Fig. 6. A multistep mechanism was used to verify the effectiveness of the proposed method.

4.3. Results of SSA and data conversion

First, SSA was used for the embedding, SVD, and reconstruction of

Table 3
Error comparison with several popular models without SSA for various time horizons.

		Error	RBF	ELM	SVR	WNN	HLNN	OTSTA-SSA-HLNN
Experiment I	One-step ahead	MAE(%)	8.3678	6.2961	6.2978	6.4827	6.2396	4.0495
		RMSE(%)	11.3944	10.8141	10.9101	10.9988	10.7386	6.8763
	Three-step ahead	MAE(%)	9.3474	6.8102	6.7023	6.8812	6.6527	4.2188
		RMSE(%)	13.3314	11.2210	11.7982	11.4633	11.4325	7.0088
	Six-step ahead	MAE(%)	11.8019	8.9022	9.0021	9.3412	8.8210	6.1927
		RMSE(%)	14.9285	12.3631	12.7964	13.7302	12.0216	9.6154
	Twelve-step ahead	MAE(%)	17.0124	12.4413	12.6601	12.2987	12.3158	10.0026
		RMSE(%)	21.1986	16.1415	16.2952	17.3819	15.9965	13.4024
Experiment II	One-step ahead	MAE(%)	8.1191	6.9919	6.5126	6.9818	6.3562	4.0521
		RMSE(%)	13.8777	11.5681	11.9421	12.5167	11.8810	6.9244
	Three-step ahead	MAE(%)	10.3279	7.9027	6.7735	7.7839	7.0124	4.1579
		RMSE(%)	14.5732	12.0088	11.8253	13.1398	11.4231	7.0752
	Six-step ahead	MAE(%)	12.7888	9.3704	9.3145	9.8956	9.3923	6.2123
		RMSE(%)	15.5378	13.6719	13.3991	14.2844	12.8124	9.5912
	Twelve-step ahead	MAE(%)	17.2964	12.8416	12.1617	12.9094	12.1106	9.9126
		RMSE(%)	21.8356	16.2669	15.8307	16.4710	15.7165	13.8812

Table 4
Error comparison with several popular models with SSA for various time horizons.

		Error	SSA-RBF	SSA-ELM	SSA-SVR	SSA-WNN	SSA-HLNN	OTSTA-SSA-HLNN
Experiment I	One-step ahead	MAE(%)	7.5243	5.3253	5.2134	5.6624	5.3214	4.0495
		RMSE(%)	10.0369	7.9986	8.0125	8.1256	8.0124	6.8763
	Three-step ahead	MAE(%)	8.0359	5.7965	5.8261	5.9943	5.6235	4.2188
		RMSE(%)	11.0022	9.0124	9.1258	9.2564	9.4985	7.0088
	Six-step ahead	MAE(%)	10.6657	7.2114	6.9217	7.1264	6.8320	6.1927
		RMSE(%)	13.9621	10.9985	10.6783	11.2598	11.5341	9.6154
	Twelve-step ahead	MAE(%)	16.2452	11.3867	11.1251	11.4236	11.2891	10.0026
		RMSE(%)	19.8824	14.9968	13.9986	14.9963	15.0031	13.4024
Experiment II	One-step ahead	MAE(%)	7.7454	6.0124	5.6214	5.6892	5.4021	4.0521
		RMSE(%)	10.1214	8.2926	8.1123	9.0213	8.3124	6.9244
	Three-step ahead	MAE(%)	8.9092	6.3933	6.2214	6.4245	5.7275	4.1579
		RMSE(%)	12.1187	9.2123	9.0892	10.0467	9.6253	7.0752
	Six-step ahead	MAE(%)	11.4786	7.0452	7.0765	7.2989	7.8782	6.2123
		RMSE(%)	14.0899	10.8994	10.8769	11.5216	10.6301	9.5912
	Twelve-step ahead	MAE(%)	16.3769	11.1608	11.9912	12.0618	11.1923	9.9126
		RMSE(%)	20.0213	15.0234	13.9014	15.1210	14.9910	13.8812

the wind power series. The SSA parameter L must be within $2 \leqslant L \leqslant \frac{N-1}{2}$ [30]. Sampling was conducted every 10 min, thus obtaining six samples per hour ($n = 6$); for experiment I, $L_1 = \frac{5184}{24\times 6} = 36$, and for experiment II, $L_2 = \frac{5760}{24\times 6} = 40$. On the basis of the component contribution for original wind power series, the wind power series was decomposed as trend and harmonic wind power time series, namely, behavior and noise. Fig. 7 shows the decomposed wind power time series.

Then, the positive and negative conversions of the decomposed signals were calculated. Figs. 8 and 9 show the results of two positive and two negative decomposed signals.

4.4. Forecasting results and discussion

The proposed method was used to forecast wind power in this section. We verified the effectiveness of the proposed method compared with other forecasting methods in previous references.

4.4.1. Discussion of forecasting model input

To illustrate the input of the forecasting model, various model inputs were selected to forecast the wind power series. Multi-input forecasting models were used. Fig. 10 and Table 1 present the corresponding errors. Fig. 10(a) shows the MAE and RMSE histograms of experiment I, and Fig. 10(b) displays the MAE and RMSE histograms of experiment **II**.

Fig. 10(a) and 10(b) show that the MAE and RMSE of the proposed six- and nine-input models are smaller than those of the other input models. It can be seen from Table 1 that: For experiment I, the forecasting model with nine inputs has the lowest MAE values in 1-, 3-, 6-, and 12-step ahead forecasting, whereas the model with six inputs has the lowest RMSE values in 1-, 3-, and 6-step ahead forecasting. Only the MAE values of the six-input model are slightly higher than those of the nine-input model. For experiment II, the forecasting model with nine inputs has the lowest MAE values in six-step ahead forecasting, whereas the model with six inputs has the lowest MAE values in 1-, 3-, and 12-step ahead forecasting. Only the RMSE values of the six-input model are slightly higher than those of the nine-input model in 12-step ahead forecasting. The MAE and RMSE of the proposed method obtain small errors with different dataset samples, indicating the high robustness of the proposed model. Considering the structure of the forecasting model, the six-input forecasting model is preferred for wind power prediction.

4.4.2. Discussion of HLNN with OTSTA and SSA

The forecasting models were built using HLNN, OTSTA, and SSA. To verify the effectiveness of OTSTA-SSA-HLNN, it is compared with STA-SSA-HLNN, SSA-HLNN, and HLNN. Table 2 shows the results of these models for multistep prediction. Fig. 11 presents the MAE and RMSE histograms of the four models.

As shown in Table 2 and Fig. 11, OTSTA-SSA-HLNN had smaller MAE and RMSE values for one-step and multistep ahead wind power forecasting. The following observations were obtained:

(1) SSA was used for data decomposition and reconstruction before

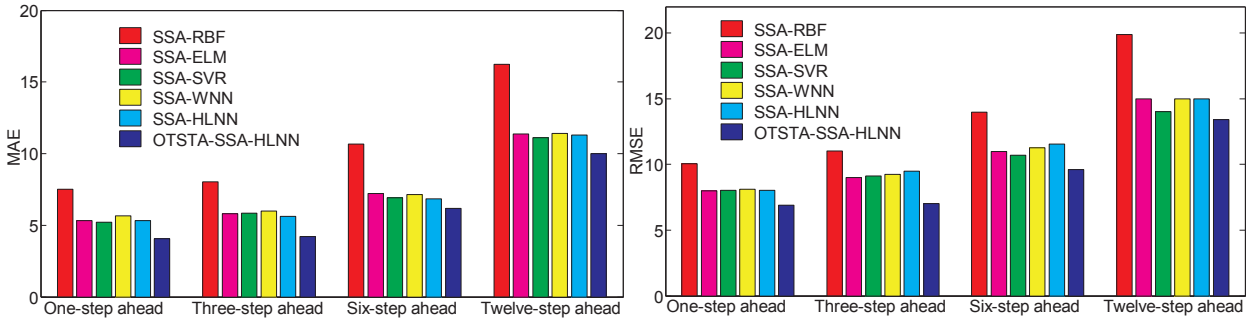

(a) MAE and RMSE histograms of experiment I

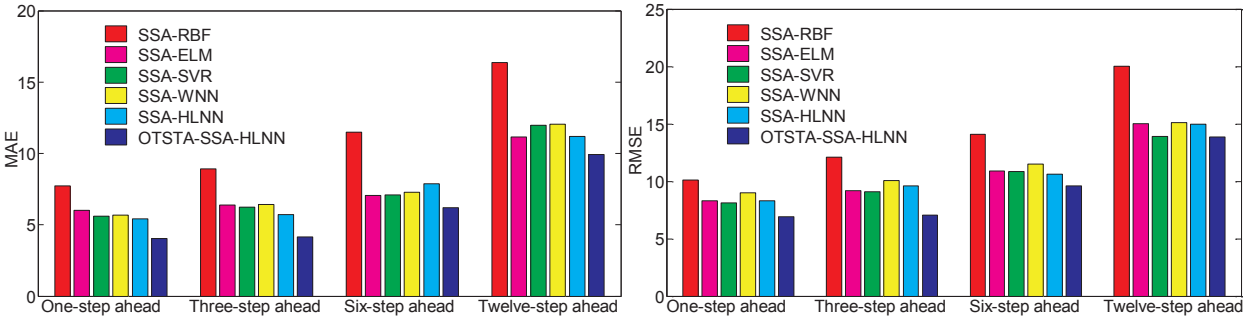

(b) MAE and RMSE histograms of experiment II

Fig. 12. Forecasting error comparison with several popular models.

Table 5
Average error comparison with several popular models for various time horizons.

Average	Error	SSA-RBF	SSA-ELM	SSA-SVR	SSA-WNN	SSA-HLNN	OTSTA-SSA-HLNN
ExperimentI	MAE(%)	10.6178	7.4300	7.2716	7.5517	7.2665	6.1159
	RMSE(%)	13.7209	10.7516	10.4538	10.9095	11.0120	9.2257
ExperimentII	MAE(%)	11.1275	7.6529	7.7276	7.8686	7.5500	6.0837
	RMSE(%)	14.0878	10.8569	10.4950	11.4277	10.8897	9.3680

forecasting, thus improving the forecasting accuracy. The forecasting results of SSA-HLNN have higher accuracy than HLNN. For experiment I, the MAE value decreased by 0.9182% and RMSE decreased by 2.7262% for one-step ahead forecasting. The MAE value decreased by 1.0292% and RMSE decreased by 1.934% for three-step ahead forecasting. The MAE value decreased by 1.989% and RMSE decreased by 0.4875% for six-step ahead forecasting. The MAE value decreased by 1.0267% and RMSE decreased by 0.9934% for 12-step ahead forecasting. For experiment II, only HLNN had a large error. Hence, SSA can improve the forecasting accuracy.

(2) The weight of STA-SAA-HLNN forecasting model was optimized using the STA optimization algorithm. The results showed that the optimized model had higher accuracy and smaller MAE and RMSE values than the SAA-HLNN model. Specifically, the accuracy of 12-step ahead forecasting was greatly improved.

(3) As a swarm intelligence algorithm, STA has the disadvantage of easily falling into the local optimum. The OTSTA-SSA-HLNN model optimized by OTSTA had better forecasting results than the STA-SAA-HLNN model. One-step and multistep ahead forecasting had small MAE values. For one-, three-, and nine-step ahead forecasting, the OTSTA-SSA-HLNN model had small RMSE value, whereas 12-step ahead forecasting had high RMSE value.

In summary, the HLNN forecasting model combined with OTSTA and SSA has good prediction accuracy for one- and multi-step ahead wind power forecasting.

4.4.3. Comparison of results with popular forecasting models

To verify the effectiveness of the proposed OTSTA-SSA-HLNN forecasting model further, several popular wind power forecasting models, such as basic RBF [35], ELM [36], SVR [37], and WNN [38], were considered for the forecasting performance comparison. Table 3 shows the MAE and RMSE of different forecasting models without SSA. It can be seen from Table 3 that: (1) OTSTA-SSA-HLNN has the highest forecasting accuracy than other methods. (2) RBF has larger MAE and RMSE values in both one-step ahead prediction and multi-step ahead prediction. (3) On the whole, HLNN has higher forecasting accuracy than other methods, only MAE values of three-step ahead forecasting and six-step ahead forecasting of ExperimentII are higher than SVR, only MAE value of Twelve-step ahead forecasting of Experiment I are higher than WNN.

In order to hence making more robust and constructive the comparison with the proposed HLNN model, the MAE and RMSE of different forecasting models with SSA are shown in Table 4 and Fig. 12.

It can be seen from Table 4 and Fig. 12 that all methods with SSA have gotten higher forecasting accuracy. On the whole, SSA-HLNN has higher forecasting accuracy than others, only MAE values of one-step ahead forecasting and twelve-step ahead forecasting of Experiment I are higher than SSA-SVR. OTSTA-SSA-HLNN had smaller MAE and RMSE values in one- and multistep ahead forecasting than the four other methods, whereas RBF had larger MAE and RMSE values in one- and

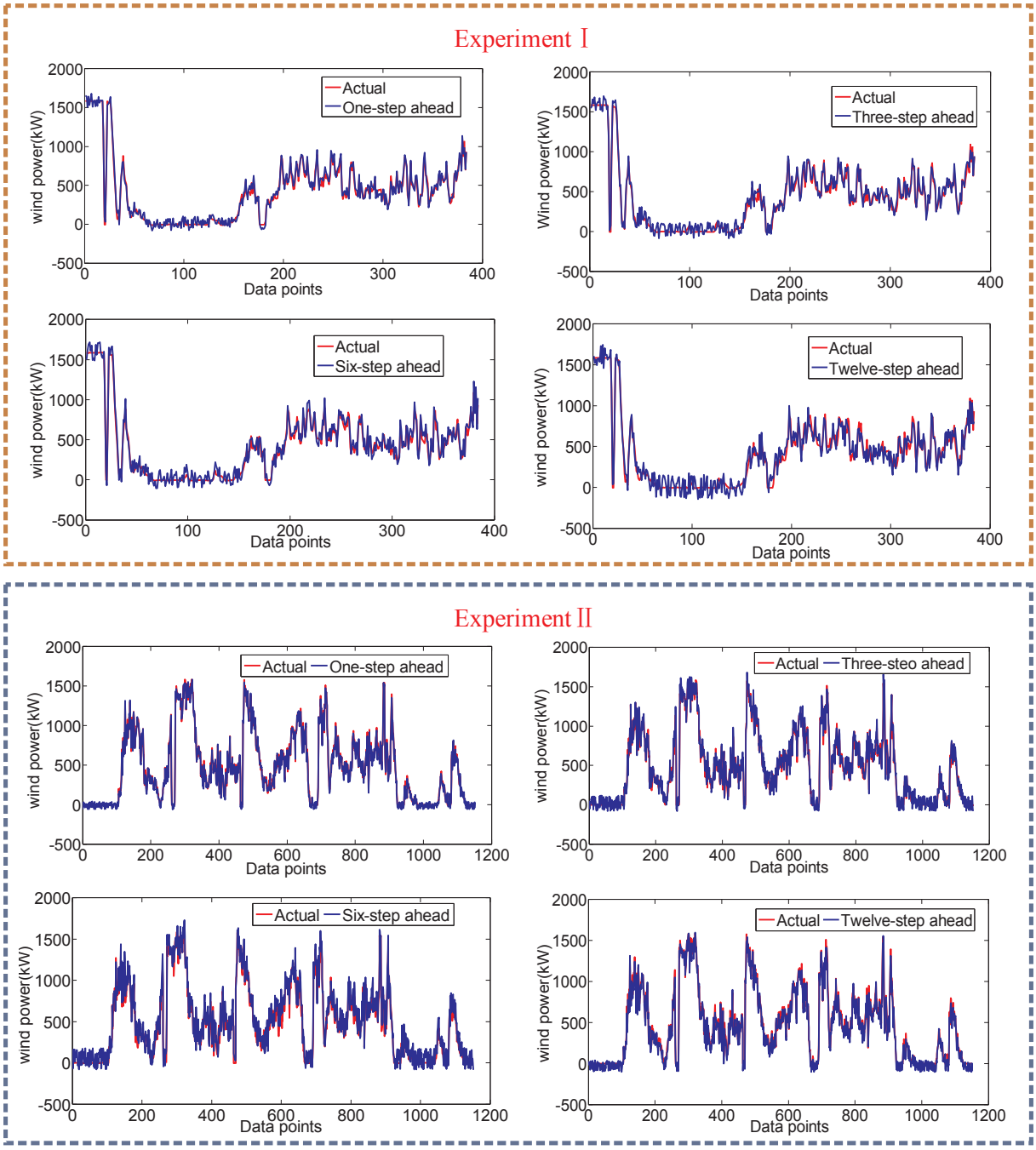

Fig. 13. Comparison of predicted values using OTSTA-SSA-HLNN with actual wind power data.

multistep ahead prediction. For experiment I, SSA-ELM, SSA-SVR and SSA-WNN have similar forecasting accuracy: (1) For 1- and 3-step ahead forecasting, SSA-ELM had the minimum RMSE values. (2) For 1-, 6-, and 12-step ahead forecasting, SSA-SVR had the minimum MAE forecasting error, whereas SSA-ELM had the minimum MAE in three-step ahead forecasting. (3) SSA-WNN had slightly higher MAE and RMSE values than the two other methods in one- and multistep forecasting. For experiment II, SSA-ELM, SSA-SVR, and SSA-WNN had similar forecasting accuracies: (1) For 1- and 3-step ahead forecasting, SSA-SVR had the minimum MAE and RMSE values. (2) For 6- and 12-step ahead forecasting, SSA-SVR had the minimum RMSE forecasting error, whereas SSA-ELM had the minimum MAE values. (3) SSA-WNN had slightly higher MAE and RMSE values than the two other methods.

Table 5 shows the average MAE and RMSE over the entire evaluation period. It can be seen form Table 5 that the average MAE values of SSA-HLNN of two experiments are all lower than SSA-WNN, SSA-SVR, SSA-ELM and SSA-RBF and the average MAE and RMSE values of the OTSTA-SAA-HLNN method leads to the lowest average errors for 12-step ahead forecasting over the entire evaluation period. For experiment I, the average MAE value of OTSTA-SSA-HLNN was 6.1159%, which was considerably below the 1.4358%, 1.1557%, 1.3141%, and 4.5019% errors of SSA-WNN, SSA-SVR, SSA-ELM, and SSA-RBF, respectively. The average RMSE value of OTSTA-SSA-HLNN was 9.2257%, which was also considerably below the 1.6838%, 1.2281%, 1.5259%, and 4.4952% errors of SSA-WNN, SSA-SVR, SSA-ELM, and SSA-RBF, respectively. For experiment II, the average MAE value of OTSTA-SSA-HLNN was 6.0837%, which was considerably below the 1.7849%, 1.6439%, 1.5692%, and 5.0438% errors of SSA-WNN, SSA-SVR, SSA-ELM, and SSA-RBF, respectively. The average RMSE value of OTSTA-SSA-HLNN was 9.3680%, which was also considerably below

the 2.0597%, 1.1270%, 1.4889%, 4.7198% errors of SSA-WNN, SSA-SVR, SSA-ELM, and SSA-RBF, respectively. These findings indicate that OTSTA-SAA-HLNN has a good performance for multistep prediction.

Fig. 13 plots the forecasting performance of OTSTA-SSA-HLNN along with original wind time series for 1-, 3-, 6-, and 12-step ahead forecasting. Moreover, the forecasts follow the trend of the actual values closely in general for various time horizons. Fig. 13 shows that the one- and three-step ahead forecasting curves have a high degree of fitting with the actual wind power curves, which indicates the effectiveness of the proposed forecasting method. The 6- and 12-step ahead forecasting curves have certain volatility compared with the actual curve, but the volatility remains small.

Therefore, the proposed OTSTA-SSA-HLNN forecasting model has better forecasting results than popular forecasting methods, such as RBF, ELM, SVR, and WNN.

In this forecasting method, SSA was used to decompose the series into two subsequences, namely, trend and harmonic series and noise series, by reconstructing the original wind power series. Then, we calculated the positive and negative conversions of the two series, thus providing further distinctive features for the time series to improve forecast accuracy and prediction speed. For positive and negative series, Laguerre polynomial, new Laguerre polynomial, and neural network were used to build a new HLNN forecasting model. The hybrid model has two sections: type I and type II forecasting models for forecasting positive and negative series. The HLNN forecasting model not only combines the advantages of Laguerre polynomial and neural network but also has further prediction targeted for the time series. OTSTA was proposed to optimize the weights of hybrid forecasting method. A local optimal discriminant mechanism was used to judge whether state resulted in a premature phenomenon. When the algorithm resulted in a precocious phenomenon, an opposition transition learning mechanism is proposed to let algorithm jump out earliness state. OTSTA had few parameters and simple structure, as well as good convergence, which can indirectly improve the wind power forecasting accuracy.

Hence, the hybrid forecasting model has higher forecasting accuracy than other methods. A model with high forecasting accuracy has several applications. (1) The hybrid model can be used as an effective wind power forecasting strategy for wind power forecasting system, which can be applied for accurate wind power forecasting in power system control centers [11]. (2) In recent years, several effective wind turbines control methods are proposed on the premise of wind power forecasting results [39]. (3) A high wind power forecasting accuracy is good for the grid dispatching organization to enhance the competitiveness of wind energy in the electricity market and help in the formulation of scientific control strategies in wind farms [40].

5. Conclusion

High forecasting accuracy is crucial for wind power in the electricity market. A novel hybrid forecasting method based on SSA, OTSTA, and Laguerre polynomial and neural network is proposed in this paper. SSA, positive conversion, and negative conversion are applied to extract meaningful features and converse wind power series. These new positive conversion and negative series can clearly describe the sequence features. Considering the characteristics of the new positive and negative series, a hybrid Laguerre neural network forecasting model based on Laguerre polynomial and neural network is built for the series. The hybrid Laguerre neural network model has two sections: type I and type II forecasting models for forecasting positive and negative series. The corresponding forecasting model of each subsequence is built using a model with six inputs, which is more useful than other inputs. Moreover, OTSTA is proposed to optimize the weights of the hybrid forecasting method. A local optimal discriminant mechanism is used to judge whether premature phenomenon occurred. OTSTA has few parameters and simple structure, but has good convergence, which can indirectly improve the wind power forecasting accuracy.

For a fair and clear comparative study, identical test cases are applied to verify the performance of the proposed model compared with other popular methods. The results demonstrate the following: (a) The final forecasting accuracy can be improved by data with noise decomposition and reconstruction by using SSA. (b) OTSTA is helpful for strengthening the forecasting capability of the model and indirectly improving wind power forecasting accuracy. (c) The proposed hybrid Laguerre neural network model has minimum MAE and RMSE errors compared with other models. (d) The proposed forecasting model is suitable for wind power prediction.

Declaration of Competing Interest

The authors declare that they have no known competing financial interests or personal relationships that could have appeared to influence the work reported in this paper.

Acknowledgments

The work was supported by the National Natural Science Foundation of China (Grant Nos. 51767022 and 51967019), Natural Science Fund Project of Xinjiang Uygur Autonomous Region (Grant No. 2019D01C082), Science Startup Foundation of Xinjiang University for doctor, and Tianchi projection of Xinjiang Uygur Autonomous Region for doctor.

References

[1] https://wwindea.org/blog/2019/02/25/wind-power-capacity-worldwide-reaches-600-gw-539-gw-added-in-2018/.
[2] Cao Y, Liu C, Huang YH. Wind power accom-modation capability of large-scale interconnected power grid based on equivalent aggregation method. High Voltage Eng 2016;42(9):2792–9.
[3] Yang DY, Wen JX, Chan K. Smoothing and dis-patching the output of wind/battery energy storage hybrid system via model prediction control. High Voltage Eng 2017;43(3):1043–8.
[4] Foley AM, Leahy PG, Marvuglia A, McKeogh EJ. Current methods and advances in forecasting of wind power generation. Renew Energy 2012;37(1):1–8.
[5] Jung J, Broadwater RP. Current status and future advances for wind speed and power forecasting. Renew Sustain Energy Rev 2014;31:762–77.
[6] Kariniotakis G, Pinson P, Siebert N, Giebel G, Barthelmie R. The state of the art in short-term prediction of wind power - from an offshore perspective. Sea Tech Week 2004;2004:20–1.
[7] Liu H, Tian HQ, Chen C, Li YF. A hybrid statistical method to predict wind speed and wind power. Renew Energy 2010;35:1857–61.
[8] Amjady N, Keynia F, Zareipour H. Wind power prediction by a new forecast engine composed of modified hybrid neural network and enhanced particle swarm optimization. IEEE Trans Sustain Energy 2011;2:265–76.
[9] Hong YY, Chang HL, Chiu CS. Hour-ahead wind power and speed forecasting using simultaneous perturbation stochastic approximation (SPSA) algorithm and neural network with fuzzy inputs. Energy 2010;35:3870–6.
[10] Zhang X, Wang J, Zhang K. Short-term electric load forecasting based on singular spectrum analysis and support vector machine optimized by Cuckoo search algorithm. Electr Power Syst Res 2017;146:270–85.
[11] Sharifian A, Ghadi MJ, Ghavidel S, Li L, Zhang JF. A new method based on Type-2 fuzzy neural network for accurate wind power forecasting under uncertain data. Renew Energy 2018;120:220–30.
[12] Lin Y, Yang M, Wan C, Wang JH, Song YH. A multi-model combination approach for probabilistic wind power forecasting. IEEE Trans Sustain Energy 2018;10(1):226–37.
[13] Wang Z, Shen C, Liu F. A conditional model of wind power forecast errors and its application in scenario generation. Appl Energy 2018;212:771–85.
[14] López E, Valle C, Allende H, Gil E, Madsen H. Wind power forecasting based on echo state networks and long short-term memory. Energies 2018;11(3):526.
[15] Wang Y, Hu Q, Srinivasan D, Wang Z. Wind power curve modeling and wind power forecasting with inconsistent data. IEEE Trans Sustain Energy 2018;10(1):16–25.
[16] Afshari IM, Niknam T, Khooban MH. Probabilistic wind power forecasting using a novel hybrid intelligent method. Neural Comput Appl 2018;30(2):473–85.
[17] Jiao R, Huang X, Ma X, Han LY, Tian W. A model combining stacked auto encoder and back propagation algorithm for short-term wind power forecasting. IEEE Access 2018;6:17851–8.
[18] Zjavka L, Mišák S. Direct wind power forecasting using a polynomial decomposition of the general differential equation. IEEE Trans Sustain Energy 2018;9(4):1529–39.
[19] Yu R, Gao J, Yu M, Lu WH, Xu TY, Zhao MK, et al. LSTM-EFG for wind power forecasting based on sequential correlation features. Future Generation Com Sys 2019;93:33–42.
[20] Niu DX, Pu D, Dai SY. Ultra-short-term wind-power forecasting based on the

weighted random forest optimized by the niche immune lion algorithm. Energies 2018;11(5):1098.
[21] Zhang YC, Le J, Liao XB, Zheng F, Li YH. A novel combination forecasting model for wind power integrating least square support vector machine, deep belief network, singular spectrum analysis and locality-sensitive hashing. Energy 2019;168:558–72.
[22] Lu P, Ye L, Sun BH, Zhang CH, Zhao YN. A new hybrid prediction method of ultra-short-term wind power forecasting based on EEMD-PE and LSSVM optimized by the GSA. Energies 2018;11(4):697.
[23] Naik J, Dash S, Dash PK, Bisoi R. Short term wind power forecasting using hybrid variational mode decomposition and multi-kernel regularized pseudo inverse neural network. Renew Energy 2018;118:180–212.
[24] Du P, Wang J, Yang W, Yang WD, Niu T. A novel hybrid model for short-term wind power forecasting. Appl Soft Comput 2019;80:93–106.
[25] Zhou J, Yu XC, Jin BL. Short-term wind power forecasting: A new hybrid model combined extreme-point symmetric mode decomposition, extreme learning machine and particle swarm optimization. Sustainability 2018;10(9):3202.
[26] Wang KJ, Qi XX, Liu HD, Song JK. Deep belief network based k-means cluster approach for short-term wind power forecasting. Energy 2018;165:840–52.
[27] Leng H, Li XR, Zhu JR, Tang HG, Zhang ZD, Ghadimi N. A new wind power prediction method based on ridgelet transforms, hybrid feature selection and closed-loop forecasting. Adv Eng Inf 2018;36:20–30.
[28] Wang C, Zhang H, Fan W, Ma P. A new chaotic time series hybrid prediction method of wind power based on EEMD-SE and full-parameters continued fraction. Energy 2017;138:977–90.
[29] Moreno SR, dos Santos Coelho L. Wind speed forecasting approach based on singular spectrum analysis and adaptive neuro fuzzy inference system. Renew Energy 2018;126:736–54.
[30] Golyandina N, Nekrutkin V, Zhigljavsky AA. Analysis of time series structure: SSA and related techniques. New York-London: Chapman & Hall/CRC; 2001.
[31] Zhang Y, Zhong T, Li W. Laguerre orthogonal basis feed-forward neural network with its weights determined directly. J Jinan University (Natural Science Edition) 2008;29(3):249–53.
[32] Zhou XJ, Yang CH, Gui WH. Initial version of state transition algorithm. 2012 Third International Conference on Digital Manufacturing & automation 2012:644–7.
[33] Wang C, Zhang H, Fan W. A new wind power prediction method based on chaotic theory and Bernstein Neural Network. Energy 2016;117:259–71.
[34] Wang J, Li Y. Multi-step ahead wind speed prediction based on optimal feature extraction, long short term memory neural network and error correction strategy. Appl Energy 2018;230:429–43.
[35] Park J, Sandberg IW. Universal approximation using radial-basis-function networks. Neural Comput 1991;3:246–57.
[36] Huang GB, Zhu QY. Extreme learning machine: theory and applications. Neurocomputing 2006;70:489–501.
[37] Zhang H, Chen LX, Qu Y, Zhao G, Guo ZW. Support vector regression based on grid-search method for short-term wind power forecasting. J Appl Math 2014;2014:1–11.
[38] Chitsaz H, Amjady N, Zareipour H. Wind power forecast using wavelet neural network trained by improved clonal selection algorithm. Energy Convers Manage 2015;89:588–98.
[39] Song DR, Fan XY, Yang J, Liu AF, Chen SF, Joo YH. Power extraction efficiency optimization of horizontal-axis wind turbines through optimizing control parameters of yaw control systems using an intelligent method. Appl Energy 2018;224:267–79.
[40] Hao Y, Tian C. A novel two-stage forecasting model based on error factor and ensemble method for multi-step wind power forecasting. Appl Energy 2019;238:368–83.